the FEBS Journal

Functional analysis of the methylmalonyl-CoA epimerase from *Caenorhabditis elegans*

Jochen Kühnl[1], Thomas Bobik[2], James B Procter[3], Cora Burmeister[1], Jana Höppner[1], Inga Wilde[1], Kai Lüersen[1], Andrew E. Torda[3], Rolf D. Walter[1] and Eva Liebau[1]

1 Department of Biochemistry, Bernhard-Nocht-Institute for Tropical Medicine, Hamburg, Germany
2 Department of Biochemistry, Biophysics and Molecular Biology, Iowa State University, Ames, IA, USA
3 Centre of Bioinformatics, University of Hamburg, Germany

Keywords
Caenorhabditis elegans; epimerase; methylmalonyl-CoA

Correspondence
E. Liebau, Department of Biochemistry, Bernhard-Nocht-Institute for Tropical Medicine, Bernhard-Nocht-Str. 74, D-20359 Hamburg, Germany
Fax: +49 40 42818 418
Tel: +49 40 42818 415
E-mail: liebau@bni.uni-hamburg.de

Note
The nucleotide sequence data reported in this paper have been submitted to the GenBank data base with the accession number AY594301 (UniProt P90791).

(Received 5 October 2004, revised 18 January 2005, accepted 21 January 2005)

doi:10.1111/j.1742-4658.2005.04579.x

Methylmalonyl-CoA epimerase (MCE) is an enzyme involved in the propionyl-CoA metabolism that is responsible for the degradation of branched amino acids and odd-chain fatty acids. This pathway typically functions in the reversible conversion of propionyl-CoA to succinyl-CoA. The *Caenorhabditis elegans* genome contains a single gene encoding MCE (*mce-1*) corresponding to a 15 kDa protein. This was expressed in *Escherichia coli* and the enzymatic activity was determined. Analysis of the protein expression pattern at both the tissue and subcellular level by microinjection of green fluorescent protein constructs revealed expression in the pharynx, hypodermis and, most prominently in body wall muscles. The subcellular pattern agrees with predictions of mitochondrial localization. The sequence similarity to an MCE of known structure was high enough to permit a three-dimensional model to be built, suggesting conservation of ligand and metal binding sites. Comparison with corresponding sequences from a variety of organisms shows more than 1/6 of the sequence is completely conserved. Mutants allelic to *mce-1* showed no obvious phenotypic alterations, demonstrating that the enzyme is not essential for normal worm development under laboratory conditions. However, survival of the knockout mutants was altered when exposed to stress conditions, with mutants surprisingly showing an increased resistance to oxidative stress.

Methylmalonyl-CoA epimerase (MCE; EC 5.1.99.1) belongs to the vicinal-oxygen-chelate superfamily (VOC), whose members are structurally related proteins that are able to catalyse a large range of divalent metal ion-dependent reactions involving stabilization of the respective oxyanion intermediates. All members possess a characteristic common structural scaffold, comprised of βαβββ modules, two of these usually forming a metal-binding/active site [1]. However, assembly of the domains occurs in several different ways, suggesting that the evolution of these proteins probably involved multiple gene duplication, gene fusion and domain swapping events. Members of the family include the Fe(II)-dependent extradiol dioxygenase, a Mn(II)-containing glutathione *S*-transferase (GST) that inactivates fosfomycin, the bleomycin-resistance protein, the Zn(II)-dependent glyoxalase I and the Co(II)-dependent MCE [2,3].

MCE is an enzyme involved in propionyl-CoA metabolism, a pathway responsible for the degradation of branched amino acids and odd chain fatty acids. The propionyl-CoA carboxylase catalyses the formation of the S-epimer of methylmalonyl-CoA. For further catalysis by the vitamin B12-dependent

Abbreviations
Cbl, cobalamin; MCE, methylmalonyl-CoA epimerase; MCM, methylmalonyl-CoA mutase; MMA, methylmalonic aciduria; GFP, green fluorescent protein.

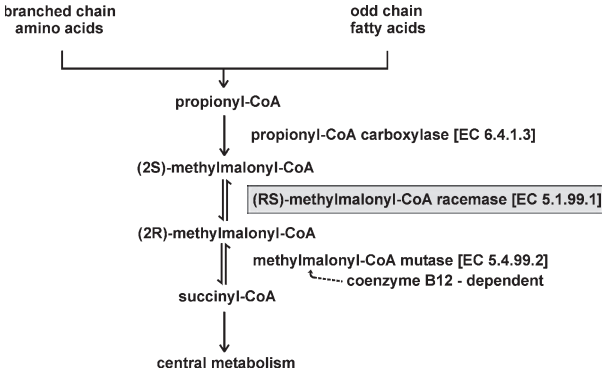

Fig. 1. Coenzyme B_{12}-dependent propionyl CoA dependent pathway. The first step in handling the three-carbon propionyl-CoA is carboxylation by the biotin-dependent propionyl-CoA carboxylase in an ATP-requiring reaction. The *S*-enantiomer of methylmalonyl-CoA is then converted to the *R*-enantiomer by the *RS*-methylmalonyl-CoA epimerase. In the final step, the *R*-enantiomer is converted to succinyl-CoA by coenzyme B_{12}-dependent methylmalonyl-CoA mutase. Succinyl-CoA can then be metabolized through the tricarboxylic acid cycle.

methylmalonyl-CoA mutase (MCM), the chiral molecule must be in its correct isomeric form. This epimerization is carried out by the MCE (Fig. 1). Defects in methylmalonyl-CoA metabolism cause methylmalonic aciduria (MMA), a rare disorder that is associated with infant mortality and developmental retardation [4]. It is still a matter of debate, whether methylmalonic acid is the main neurotoxic metabolite causing these pathological changes via inhibition of mitochondrial energy metabolism [5] or whether they are caused by 'metabolic stroke' due to accumulating toxic organic acids. It has also been shown that neuronal damage is mainly driven via metabolites that derive from alternative oxidation pathways of propionyl-CoA, in particular 2-methylcitric acid, malonic acid, and propionyl-CoA [6].

MCEs have been purified from rat, sheep, *Propionibacterium shermanii* and *Pyrococcus horikoshii*. Furthermore, the human [7], *P. horikoshii* and *P. shermanii* MCE have been recombinantly expressed in *Escherichia coli* [8]. Among the prokaryotes, MCEs are involved in autotrophic CO_2 fixation via the 3-hydroxypropionate pathway and in propionate fermentation [9]. In the methylotrophic bacterium *Methylobacterium extorquens*, MCE is part of the glyoxylate regeneration pathway, an essential element of methylotrophic metabolism [10]. Additionally, *S*-methylmalonyl-CoA is the precursor of polyketides, antibiotics that span a broad range of therapeutic areas. Heterologous production of polyketides was achieved in *E. coli*, lacking needed acyl-CoA precursors, by introducing the methylmalonyl-CoA mutase-epimerase pathway and feeding the bacteria with propionate and hydroxocobalamin [11,12].

Caenorhabditis elegans was chosen as a model system to elucidate the properties and functions of MCE because genetic and transgenic techniques in this context are well developed and the system lends itself to study under normal and stress conditions. A BLAST [13] search of the *C. elegans* genome identified only one potential MCE gene (*mce-1*). In this paper we present a detailed study of the structure and expression of the *mce-1* gene in *C. elegans*.

Results and Discussion

Identification and sequence analysis of *C. elegans* MCE

Searches in the *C. elegans* databases [14–16] identified D2030.5 with a conceptual open reading frame for MCE (*mce-1*). The gene of 906 bp, is localized on chromosome I and is composed of three exons with two intervening sequences (Fig. 2). The complete cDNA sequence, as well as the start of transcription were determined by RT-PCR and DNA sequencing (Fig. 3). The message possesses a 5′-spliced leader (SL1) sequence, followed by 17 nucleotides before the initiation codon AUG at nucleotide 40. The cDNA sequence confirmed the intron-exon boundaries of all three exons predicted from the genomic sequence in the worm database. When comparing the cDNA sequence with the genomic DNA exons for nucleotide differences, no changes were observed. The 489 bp

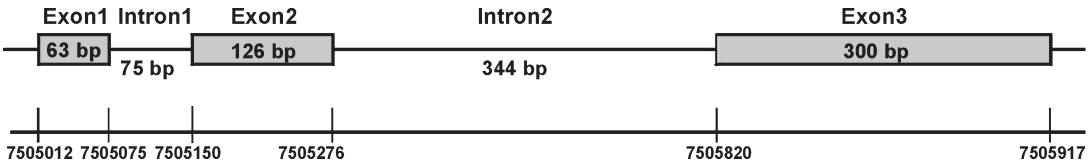

Fig. 2. Structural organization of the *mce-1* from *C. elegans*. Exons are indicated by boxes, whereas introns are symbolized by lines. The chromosomal localization is given below.

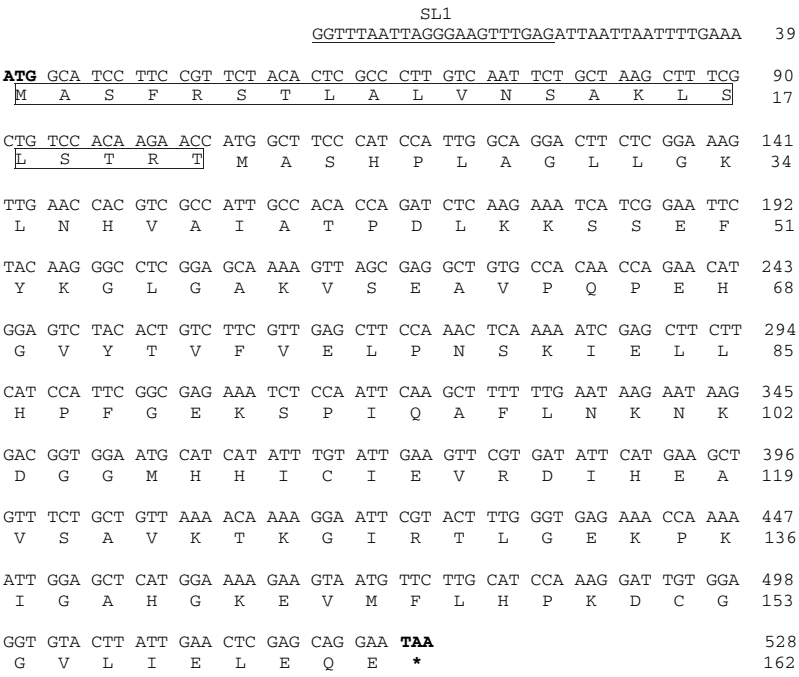

Fig. 3. Nucleotide and deduced amino acid sequence of the MCE-1 from *C. elegans*. Initiation and termination codons are shown in bold. The spliced leader 1 (SL1) site is underlined and the mitochondrial leader sequence is boxed.

cDNA possesses a 162 amino acid open reading frame with a calculated mass of 17.6 kDa.

Figure 4 shows a multiple sequence alignment of MCE-1 from *C. elegans* with the available prokaryotic and eukaryotic MCEs. Like the human and mouse sequences, the *C. elegans* sequence has additional N-terminal 22 residues for mitochondrial targeting with the peptide being cleaved once the protein has reached its target. This targeting is supported by results from the MITOPROT server which suggests a 95% chance of mitochondrial localization [17,18]. The multiple sequence alignment also shows 23 amino acids which are conserved across all organisms and the sequence similarity to human, mouse and *M. extorquens* counterparts is very high (over 65% sequence identity). In contrast the relationship to MCE from *P. shermanii*, *P. abyssi* and *P. horikoshii* MCE is much more distant (sequence identity near 30%). Other members of the VOC superfamily are even more remote (Fig. 5) with sequence identity less than 25%.

Homology model

The three dimensional model of MCE-1 (Fig. 6) was based on the structure of the corresponding enzyme from *P. shermanii* [19]. Although the sequence homology is not high, the proteins are of similar size and the alignment suggests the template has only a single small insertion of six residues. Most importantly, the model serves to locate some of the functionally important residues. As described for the *P. shermanii* enzyme, the MCE-1 monomer from *C. elegans* is folded into two tandem βαβββ modules each spanning around 60 amino acid residues. Within the two modules, the connectivity of the strands are β_1, β_4, β_3, β_2 and β_5, β_8, β_6, β_7. They pack edge-to-edge to create an eight-stranded β-sheet that curves around to create a cleft, with the first strand of the N-terminal module antiparallel to the first strand of the C-terminal module. At the bottom of this U-shaped cavity is the metal binding site, where the divalent metal ion binds. In MCE-1, the metal ion is coordinated to the side chains of His15, Glu61, His86 and Glu136, the binding to the same residues occuring in pairs at equivalent positions along strands β_1 and β_4 (Fig. 6).

These positions correspond to the metal binding ligand positions of other members of the VOC superfamily. Superimposing *P. shermanii* MCE on the human glyoxalase structure shows that the Co^{2+} ion of the MCE is only 0.2 Å from the position of the Zn^{2+} ion in the glyoxalase [19] and it was suggested that the formation of a symmetric, oligomeric protein with the ability to bind a metal ion via four side chains was a crucial step in the evolution of the modern VOC superfamily [20].

Biochemical evidence suggests the participation of two active site functional groups that act as acid/base catalysts in the epimerization reaction [21], wherein one base abstracts the C2 proton of the S-epimer of methylmalonyl-CoA, the C2 configuration inverts and

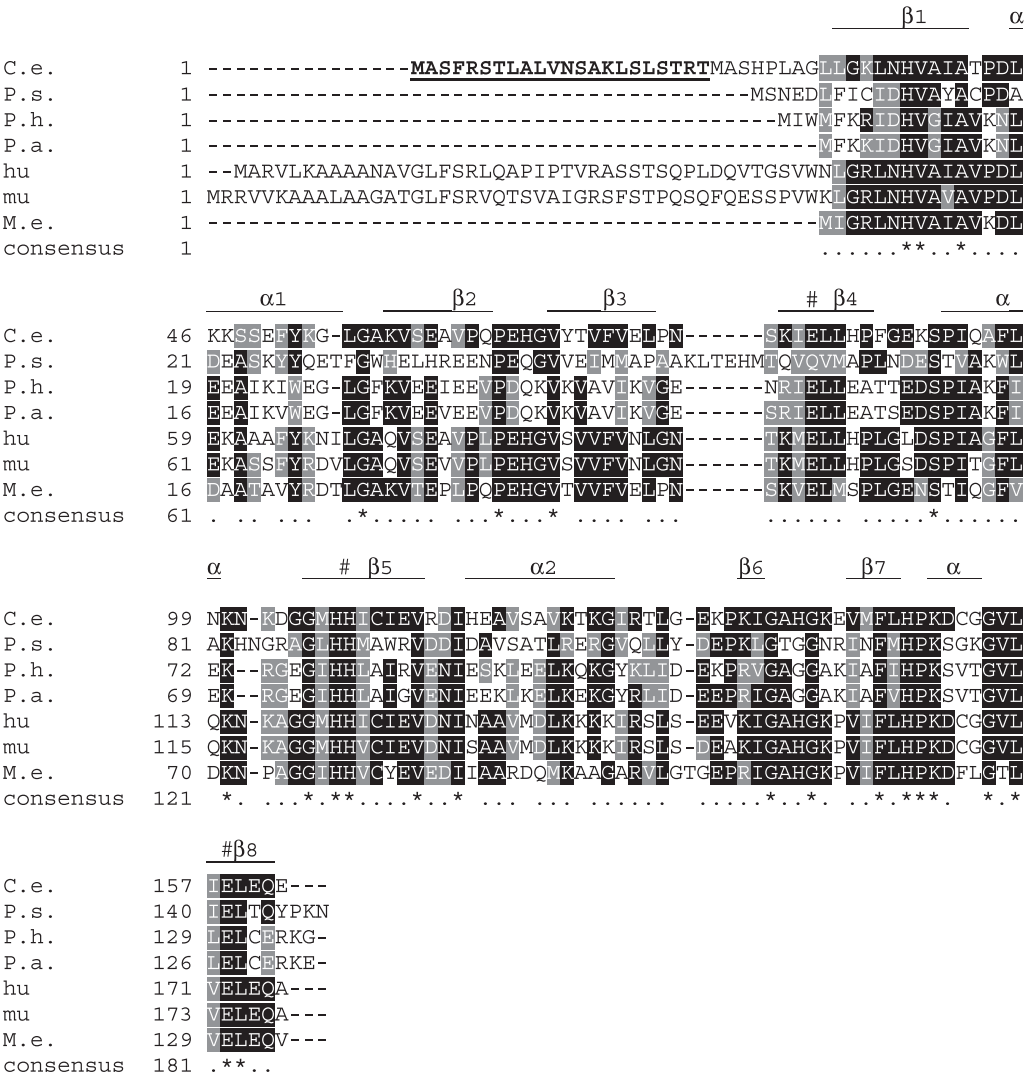

Fig. 4. Alignment of known MCE sequences. C.e., *Caenorhabditis elegans* (P90791); P.s., *Propionibakterium shermanii* (Q8VQN0); P.h., *Pyrococcus horikoshii* (Q977P4); P.a., *Pyrococcus abyssi* (Q9V226); hu, human MCE (Q96PE7), mu, mouse MCE (Q9D1I5), M.e., *Methylobacterium extorquens* (Q84FV9); gaps are indicated by the dash (–). The star (*) indicates identical, the dot (.), homologous amino acids. The mitochondrial leader sequence of the MCE from *C. elegans* is in bold and underlined. Amino acids responsible for cobalt binding are indicated with '#'. Bars indicate the secondary structure of the MCE from *P. shermanii* with 'β' for β-sheets and 'α' for α-helices.

the conjugate acid of a second symmetrically related base, provided by the second βαβββ motif, donates a proton to C2. Substrate binding to a metal stabilizes the anionic intermediate. In the *P. shermanii* MCE, the metal binding site is provided by His12, Gln65, His91 and Glu141. In the absence of crystals of an MCE-substrate complex, McCarthy *et al.* [19] modelled 2-methylmalonate into the active site of the *P. shermanii* MCE and two likely residues for the catalytic bases were identified: Glu48 in position to abstract the proton and Glu141 in position to donate the proton. Whereas Glu141 is conserved in all known MCE sequences, Glu48 is replaced by threonine or valine in all other known MCE sequences (Fig. 4); here the glutamine ligand that is *trans* to Glu141 (Gln65 in *P. shermanii* MCE) is replaced by a glutamate, allowing the noncoordinated carboxyl oxygen to act as the base instead.

Epimerase expression, purification and assay

Protein expression by an *E. coli* strain constructed to produce high levels of the MCE-1 and by a control strain (plasmid without insert) were analyzed by SDS/PAGE (Fig. 7). Large amounts of a protein with a molecular mass of around 20 kDa were produced

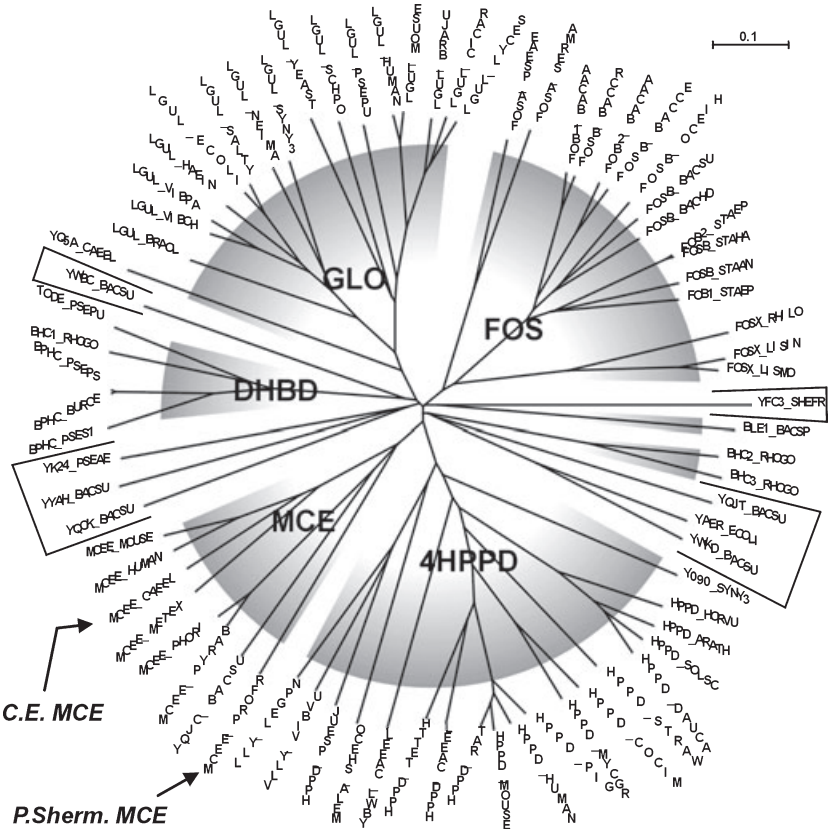

Fig. 5. Unrooted phylogeny for the VOC superfamily. Shaded segments of the tree highlight clades containing sequences with a common, characterized function. Branches to sequences with unknown function are unshaded and their leaves outlined in black. The major functional classes are labeled as: MCE, methylmalonyl-CoA epimerase; GLO, glyoxalase I; FOS, fosfomycin resistance; DHBD, extradiol-oxygenase (ring opening); 4HPPD, 4-hydroxy-phenylpyruvate dioxygenase. The minor functional branches are bleomycin resistance (BLE1_BACSP) and another class of extradiol-oxygenases (BHC2 and BHC3_RHOGO). The MCE-1 sequence (with a predicted swiss-prot name MCEE_CAEEL), and the structurally characterized homologue sequence from *P. Shermanii* (MCEE_PROFR) are also labeled.

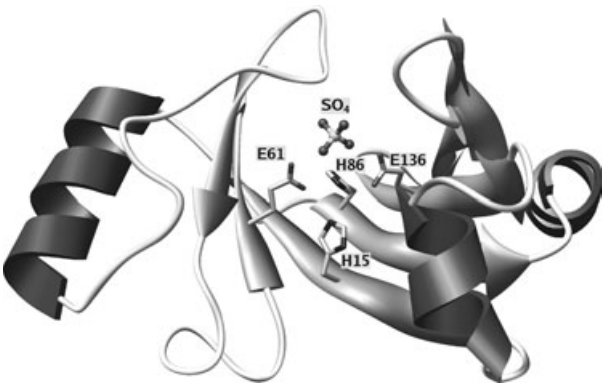

Fig. 6. Model of MCE-1 structure. View along the length of the eight-stranded beta-barrel onto the putative metal binding site involving His15, Glu61, His86 and Glu136. For comparison, the location of the sulfate ion from the parent structure (pdb 1jc4) is shown. Visualization produced with UCSF CHIMERA [34].

by the expression strain (lane 3). This is in good agreement with the predicted molecular mass of 19 kDa (15 kDa MCE-1 plus Histidine-tag, minus mitochondrial leader). In contrast, the control strain produced relatively little protein near the mass of 20 kDa (lane 2).

Nickel-affinity chromatography was used to purify the recombinant enzyme (Fig. 7, lane 4). A total of 2.1 mg MCE-1 was obtained from 28 mg of cell extract. As the epimerase was unstable, it was immediately assayed for enzymatic activity. The specific activity of the purified enzyme was 191 $\mu mol \cdot min^{-1} \cdot mg\ protein^{-1}$ and activity was dependent on the epimerase concentration. The observed epimerase activity was linear with enzyme from 0.007 to 0.016 μg of protein concentration (linear regression = 0.98). At higher enzyme concentrations, substrate concentration was limiting and activity was underestimated (data not shown).

Cell extracts from the control strain (plasmid without insert), which were processed by nickel-affinity chromatography in parallel with the expression strain, lacked detectable epimerase activity. The assay employed was a linked assay that requires MCM. As expected, no epimerase activity was observed when MCM, or coenzyme B12 was omitted from the assay mixtures (data not shown). These controls eliminated the possibility that the epimerase preparation contained an activity that acted directly on methylmalonyl-CoA. This is of potential concern, as the activity of the epimerase in the crude cell extract could not be measured due to a methylmalonyl-CoA hydrolase

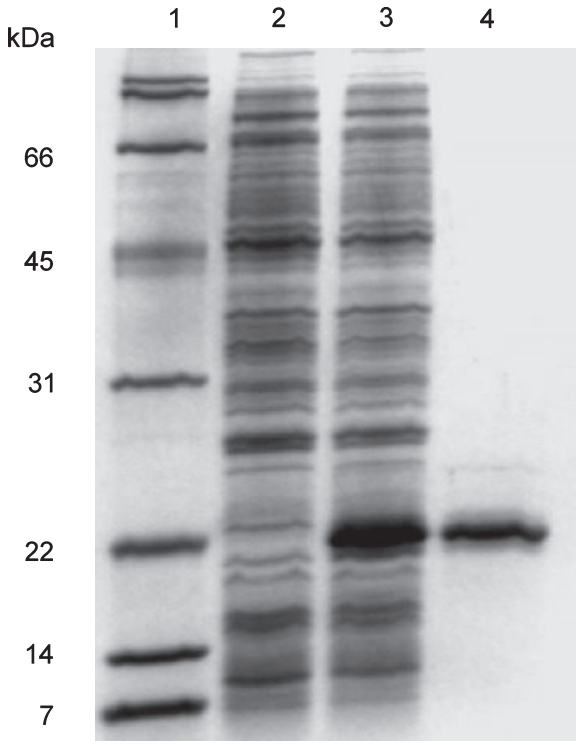

Fig. 7. Expression and purification of the MCE-1. SDS/PAGE was used to analyse the expression and purification of the epimerase. Lane 1, molecular mass markers containing galactosidase (116 kDa), phosphorylase B (97.4 kDa), serum albumin (66.2 kDa), ovalbumin (45.0 kDa), carbonic anhydrase (31.0 kDa), trypsin inhibitor (21.5 kDa), lysozyme (14.4 kDa), and aprotinin (6.5 kDa). Lane 2, 12 μg cell extract from control strain (vector without insert). Lane 3, 12 μg cell extract from epimerase expression strain. Lane 4, 2 μg of epimerase purified by nickel-affinity chromatography. The gel used contained 12% acrylamide.

activity which was apparently produced by the *E. coli* expression strain.

Expression pattern of mce-1::gfp fusion constructs in *C. elegans*

To determine the expression pattern of the MCE-1, a promoter reporter construct was made carrying green fluorescent protein and the MCE-1 amino acids (Met1–Val120). The subcellular distribution clearly shows that it is not distributed evenly in the tissues, but has a distinct dotted appearance, consistent with mitochondrial localization (Fig. 8B,E). The GFP-signal obtained was highly similar to the staining of Mito-Tracker Red, which specifically labels mitochondria (Fig. 8G–K). To obtain a clearer picture of the tissue localization, a construct was made with the mitochondrial target sequence completely deleted. Here, the pattern of the GFP signal indicates that MCE-1 is expressed moderately in parts of the pharynx and the hypodermis and, most prominently, in body wall muscles. The weak striations that can be observed are the result of partial exclusion of the fluorescence from the contractile elements of the muscle. Similar expression is seen in all detectable larval stages (Fig. 8D,F). Feeding of double-stranded *mce-1* RNA to the *mce-1*::gfp animals strongly inhibited GFP fluorescence (Fig. 8L,M).

Tissue distribution of MCE in eukaryotes has not been investigated. However, expression profiles of preceeding and succeeding enzymes of the pathway have been investigated. Here, the greatest quantitative activity of the coenzyme B12-dependent MCM has been found in sheep liver, correlating with the tissue distribution of vitamin B12 [22]. Furthermore, the distribution of proteins associated with vitamin B12 (or cobalamin, Cbl) has been described. Whereas for one protein the transport of Cbl into mitochondria has been proposed [23], a recent publication by Korotkova & Lidstrom (2004) [24] demonstrates functions in the protection of MCM from suicide inactivation; the other protein appears to be an adenosyltransferase [25,26]. Interestingly, highest expression of both proteins was observed in skeletal muscles and liver tissue.

Phenotypic characterization of mutants allelic to *mce-1*

The *mce-1* mutant worms show a normal phenotype with several standard tests like brood size, longevity, pharyngeal pumping, defection interval and postembryonic development (data not shown). Clearly, MCE is not essential for normal worm development under laboratory conditions. However, *mce-1* mutant worms showed an increased resistance to artificially generated reactive oxygen species. Furthermore, when comparing the resistance of mutants to wild-type worms under propionate stress conditions, the knockout mutants had an increased survival rate compared to wild-type *C. elegans* worms (Fig. 9).

The *mce-1* knockout mutants are not able to produce the R-isomer of methylmalonyl-CoA via the MCE-catalysed racemization. Whether the *S*-isomer of methylmalonyl-CoA accumulates in the *mce-1* mutant or whether it is further metabolized remains to be investigated. At this point, one can only speculate about the behaviour of the *mce-1* mutants: one possibility is the conversion of the *S*-isomer by a *S*-methylmalonyl-CoA specific hydrolase into methylmalonic acid and CoA; the existence of a hydrolase that is only

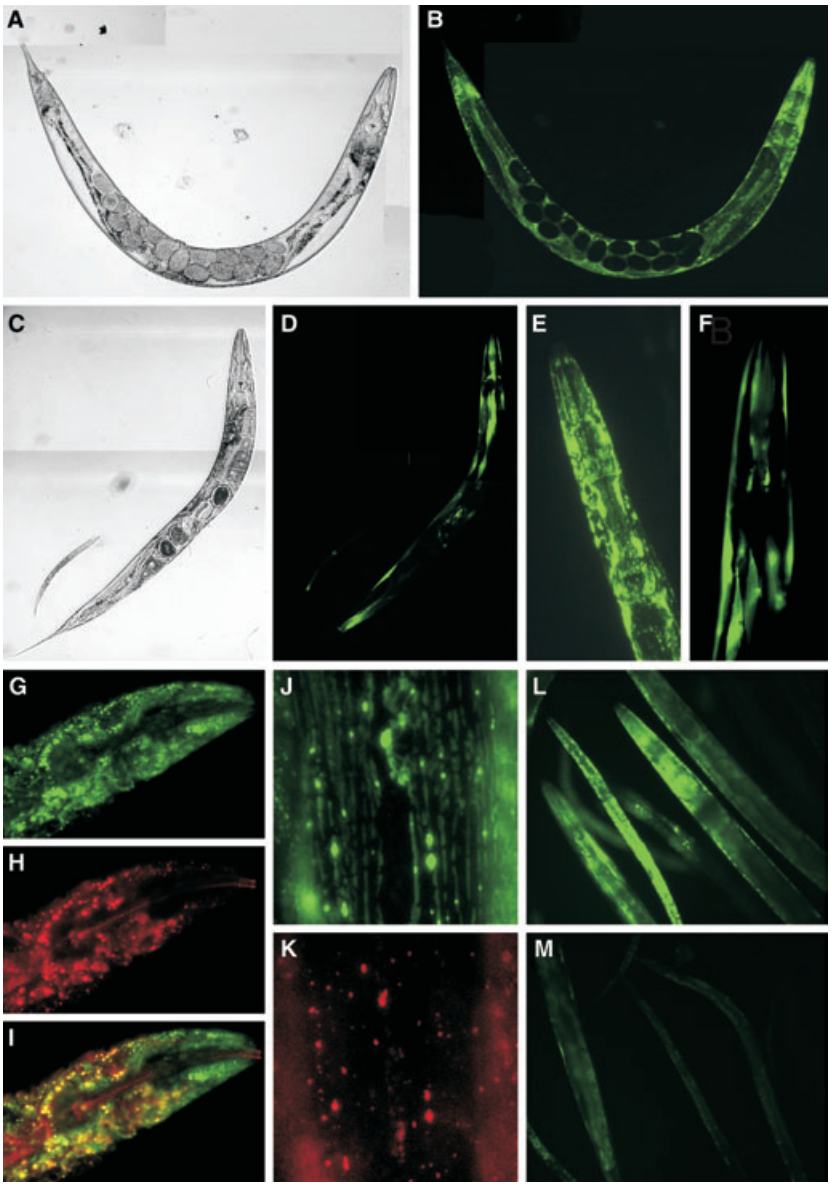

Fig. 8. Transgenic worms showing mce-1::GFP fusion protein expression. Two constructs, *mce-1*(Met1)::gfp and *mce-1*(Met23)::gfp, producing two different forms of the protein, with (A, B, E) and without (C, D, F) mitochondrial localization signal, were injected. GFP expression pattern was highly variable from animal to animal. Moderate GFP expression was observed in parts of the pharynx and the hypodermis and, most prominantly, in body wall muscles. Similar expression is seen in all detectable larval stages. With mitochondrial leader, the overall appearance was granular, the subcellular pattern of expression consistent with that of a mitochondrial enzyme. MitoTracker Red was used to confirm this mitochondrial localization (G) *mce-1*(Met1)::gfp worms (H) MitoTracker Red localization in same animal (I) merged image of (G) and (H); parallel rows of tubular mitochondria in body wall muscle (J) *mce-1*(Met1)::gfp worms and (K) MitoTracker Red localization in same animal. Treatment of *mce-1*(Met1)::gfp worms with mce-1(RNAi) effectively reduces GFP expression (L) untreated and (M) RNAi-treated worms. *C. elegans* were photographed using Nomarski optics.

active on the *S*-isomer of methylmalonyl-CoA has been isolated from rat liver [27]. Here the authors postulate that the enzyme accounts for the grossly increased amounts of methylmalonic acid that is observed during MMA. It is proposed, that the enzyme functions as an escape valve to limit the intracellular accumulation of methylmalonyl-CoA in cobalamin deficiency since methylmalonic acid can be excreted in urine and is perhaps less toxic than methylmalonyl-CoA.

Another possibility lies in the reversibility of the propionyl-CoA carboxylase reaction, converting accumulated *S*-methylmalonyl-CoA back to propionyl-CoA. However, while assessing the reversibility of the anaplerotic reactions of the propionyl-CoA pathway in hepatic biosynthetic functions and cardiac contractile activity, it was shown that in intact normal tissue, the reversibility of the propionyl-CoA carboxylase reaction is minor [28], making it unlikely that in the *mce-1* mutants the *S*-isomer is converted back to propionyl-CoA.

Finally, reversible deacylation-reacylation of methylmalonyl-CoA may function as a free methylmalonic acid shunt operating in parallel with the MCE [29] and spontaneous racemization has also been described [30]. This evidence and the fact that none of the patients with isolated MMA had a mutation in the MCE suggest that MCE-deficiency need not be associated with

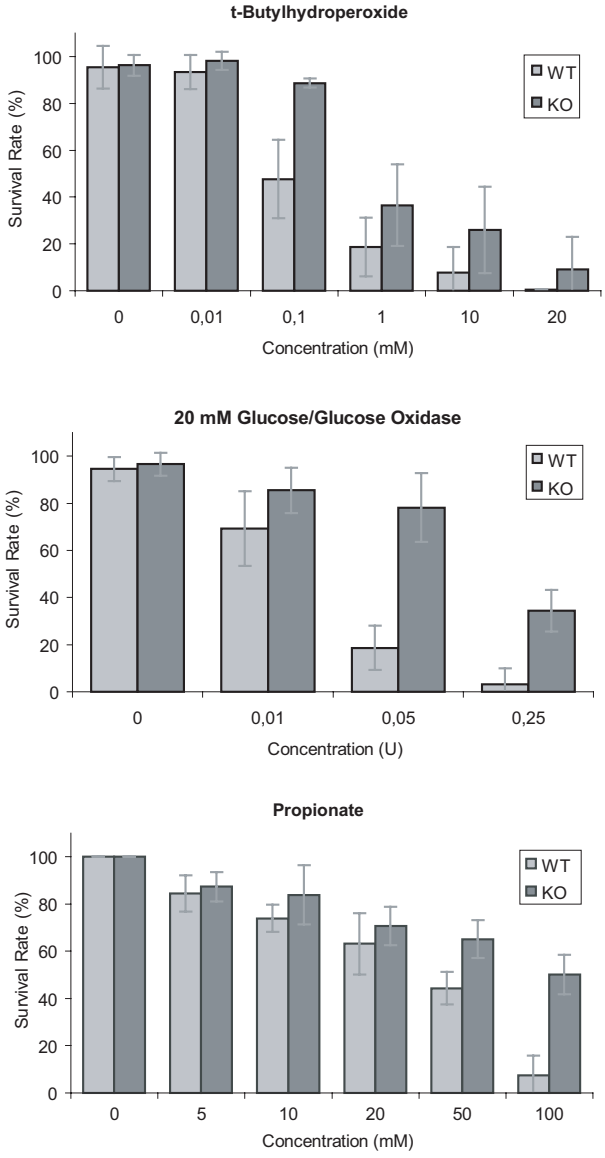

Fig. 9. Survival of the mce-1 knockout mutants under different stress conditions. Wild-type (WT) and *mce-1* mutants were cultivated in the presence of different stressor concentrations and the survival (%) of worms was determined after 2 h. The mean values were calculated from four independent experiments each with at least three survival assays using worms from different generations. *Significance based on Kruskal–Wallis test for two groups (P-value < 0.05).

symptomatic aciduria. The phenotypic analyses of the *mce-1* mutant appear to support these results.

Various animal studies have indicated that oxidative stress is involved in some organic acidurias and it is assumed that the accumulation of toxic organic acids leads to an increased production of free radicals or that the increase of metabolic by-products directly or indirectly depletes the tissue's antioxidant capacity [31].

It is difficult to explain why the *mce-1* mutants cope better under oxidative stress conditions. It is possible that, due to the missing racemization reaction catalysed by the MCE, the production of additional toxic metabolites or metabolic by-products, derived from the precursor molecule *R*-methylmalonyl CoA, is prevented. A second option is that directly or indirectly the accumulation of *S*-methylmalonyl-CoA or resulting products protect against oxidative stress or prevent further excessive production of free radicals in a not-yet-understood way. Additionally, Fontella *et al.* [32] have shown that enhanced propionic acid concentrations elicit the production of reactive oxygen species in brain tissue *in vitro*. Possibly the incubation of worms under propionate stress conditions causes a similar production of reactive oxygen species, whereby the mutant worms again cope better under these conditions. The interpretation of these observations will be clearer after further work.

A systematic RNAi screen performed by Lee *et al.* [33] identified a critical role for mitochondria in *C. elegans* longevity and, notably, 15% of the genes influencing lifespan were specific for mitochondrial functions, corresponding to a tenfold over-representation. Interestingly, some mutants and worms undergoing RNAi inactivation of several of the electron-transport chain components were more tolerant to oxidative stress treatment, using hydrogen peroxide, than control worms. The authors suggest that these RNAi clones have a lower mitochondrial membrane potential, leading to lower free radical production and it can therefore be expected that they are more resistant to additionally generated free radicals. It has been demonstrated in several studies that methylmalonic acid directly [5] or indirectly [6] – via synergistically acting alternative metabolites – inhibits the mitochondrial respiratory chain. It is then tempting to speculate, that this is the situation in the *mce-1* mutants and explains why they cope better with additionally generated reactive oxygen species.

Based on the current results, the role of MCE, at least in *C. elegans* is not clear, but the enyzme is probably not just an evolutionary relic. Not only is it present in a wide range of organisms, but more than 1/6 of the residues are conserved across a wide range of species. The observed phenotype of the *mce-1* mutants under stress condition is noteworthy and, most importantly, the close relationship of the MCE-1 from *C. elegans* to mouse and human enzymes suggests that the worm model system may help explain the role of the protein in higher organisms.

Experimental procedures

Culture conditions and nucleic acid preparation

N2 Bristol wild-type strain and LGIII, pha-1(e2123) and LGI, mce-1(ok234) were cultured in nematode growth medium [NGM: 25 mM potassium phosphate, pH 6.0, 50 mM NaCl, 0.25% (w/v) peptone, 0.5% (w/v) cholesterol, 1 mM $MgCl_2$, 1 mM $CaCl_2$] and fed with *Escherichia coli* strain OP50 (Caenorhabditis Genetics Center), grown in 3XD medium. Animals were grown at 25 °C (Bristol N2 and RB512; obtained from Caenorhabditis Genetics Center) or 15 °C (*pha-1*), respectively. For high yields, large liquid cultures were grown in bulk, followed by the removal of the bacteria by washing and floatation on sucrose gradient. Genomic DNA was prepared from worms by proteinase K digestion (Roche Applied Science, Mannheim, Germany), followed by standard phenol/chloroform extraction and ethanol precipitation. Total RNA was prepared using TRIZOL extraction according to the manufacturer's instructions (Invitrogen, Karlsruhe, Germany).

DNA sequencing

The nucleotide sequence was determined either by the Sanger dideoxy-chain-termination method on double-stranded DNA using [S^{35}]dATP and Sequenase (Amersham-Buchler, Braunschweig, Germany) or by terminator cycle sequencing using Ampli *Taq* DNA polymerase (Applied Biosystems, Darmstadt, Germany) on an Abi Prism™ automated sequencer (Perkin Elmer, Rodgau-Jügesheim, Germany).

Database search and identification of the *C. elegans* MCE

The MCE from *C. elegans* (D2030.5; *mce-1*) was identified by a blast search of wormbase [14–16] using the sequences of *Pyrococcus horikoshii* (Q977P4) and the human MCE (Q96PE7). The gene is located on chromosome I at the position 7505012–7505917 (Fig. 2). The *mce-1* cDNA clone was obtained by reverse transcription polymerase chain reaction on mRNA from mixed stage *C. elegans* cultures (strain Bristol N2). Poly(A)+ selected RNA (2 μg) were reverse transcribed using random hexamer primers. This was followed by PCR using oligo(dT) primer and the gene-specific sense primer 5′-ATGGCATCCTTCCGTTCTACA CTCGCCCTTGTC-3′. To obtain the complete 5′-end of the cDNA, the RACE (Rapid amplification of cDNA ends; Invitrogen, Karlsruhe, Germany) method was used. First strand cDNA synthesis was primed with the gene-specific antisense oligonucleotide D20/A 5′-GCCATG GTTCTTGTGGACAG-3′. Following cDNA synthesis a homopolymeric dC tail was attached and the tailed cDNA was amplified with the nested primer D20/B 5′-GCA ATGGCGACGTGGTTCAACTTTCC-3′ and the complementary homopolymer-containing anchor primer. The PCR fragment was ligated into pCR-TOPO, using the TA cloning system (Invitrogen). The *mce-1* gene and cDNA were sequenced in both directions to confirm the proposed intron-exon boundaries and the predicted amino acid sequence.

Phylogenetic analysis

A study of the VOC phylogeny was carried out, to clarify the homology between MCE and other VOC protein families. A set of VOC sequences was collected by using the MCE-1 protein sequence as a query in the CONSEQ server (BLAST *E*-value threshold 10^{-2}, Maximum number of homologs 500, five iterations) [34]. Seven sequences known to arise from shift-errors (Swiss-Prot codes of the form FUNC_ORGN_2) were removed, and the remaining 70 sequences (including the MCE-1 query) were combined with MCE sequences from human, mouse, *M. extorquens*, *P. shermanii*, *P. abyssi* and *P. horikoshii*. A multiple sequence alignment was made using MUSCLE (v 3.51) [35], with default parameters, and used to construct an unrooted phylogeny using the tree building facility of CLUSTAL-W (version 1.82) [36–38].

Homology modelling

A three-dimensional model of the MCE-1 was built based on the crystal structure of the MCE from *P. shermanii* (Protein Data Bank entry code 1jc4) [19]. Modelling followed a standard stepwise procedure. The N-terminal 22 residues (MASFRSTLALVNSAKLSLSTRT) were omitted from the model as they are a mitochondrial leader sequence typical of proteins destined for transport into mitochondria. The sequence alignment and initial coordinates were generated using WURST which combines a sequence-sequence profile alignment with structural terms [39]. Coordinates for residues in loops were generated using MODELLER 6 (v2) [40] and the final structure energy-minimized using GROMOS96 [41]. Model quality was assessed with the WHAT IF 'bump check' [42], WHAT CHECK and the 'Verify3D Structure Evaluation Server' [43].

Construction of the MCE-1 expression vector

To synthesize the *mce-1* coding region for the expression in *E. coli*, the sense primer D20C 5′-GGAATTCCA TATGGCTTCCCATCCATTGGCAGGACTTC-3′, encoding the first eight amino acid residues following the mitochondrial signal peptide and the antisense oligonucleotide D20D 5′-ATCGCGGATCCTTATTCCTGCTCGAGT TCA-3′ encoding the last six residues of the MCE-1 were used in PCR with the complete cDNA as template. The sense primer contained an *Nde*I restriction site and the anti-

sense primer a *Bam*HI restriction site (both underlined) to simplify directed, in-frame cloning into pJC40 [44]. The constructs were transformed into BL21DE3 RIL (Stratagene, La Jolla, CA, USA) and used for expression of rMCE-1. The epimerase expression strain was grown in Luria–Bertani medium supplemented with 100 $\mu g \cdot mL^{-1}$ ampicillin at 37 °C with shaking at 250 r.p.m. Cells were grown to an optical density of 0.6–0.8 at 600 nm. Then, expression of the epimerase was induced by the addition of isopropyl thio-β-D-galactoside to a final concentration of 0.5 mM. Cultures were incubated at 37 °C with shaking at 250 r.p.m. for an additional 2 h. Cells were collected by centrifugation, resuspended in 3 mL of 50 mM sodium phosphate pH 7, 300 mM NaCl, and broken using a French Pressure Cell (SLM Aminco, Urbana, IL, USA). The cell lysate was centrifuged for 30 min at 31 000 ***g*** using a Beckman JA20 rotor. The supernatant was used for protein purification.

Purification of the recombinant MCE-1 from *C. elegans*

Nickel-affinity chromatography was used to purify rMCE-1. A 1 mL Ni-nitrilotriacetic acid column (Qiagen, Chatsworth, CA, USA) was equilibrated with 10 mL of 50 mM sodium phosphate, pH 7.3. The supernatant, prepared as described above, was filtered through a 0.22 μm pore size filter, and 1 mL of filtered extract (28 mg protein) was applied to the Ni-nitrilotriacetic acid column. The column was washed with 10 mL of equilibration buffer, and 20 mL of equilibration buffer plus 40 mM imidazole. Then, the column was eluted with 3 mL of equilibration buffer containing 175 mM imidazole. The epimerase was exchanged into buffer containing 10 mM Hepes pH 7, 50 mM NaCl and 10 mM KCl, using a Vivaspin 4 centrifugal concentrator (Viva Science, Binbrook, UK).

RS-Methylmalonyl-CoA epimerase assay

RS-Methylmalonyl-CoA epimerase activity was measured using a coupled assay. In this assay, (2*S*)-methylmalonyl-CoA is converted to (2*R*)-methylmalonyl-CoA by MCE. Then (2*R*)-methylmalonyl-CoA is converted to succinyl-CoA by the coenzyme B_{12}-dependent MCM, and the MCE activity is determined by quantifying the disappearance of methylmalonyl-CoA by HPLC. As the commercially available methylmalonyl-CoA contains both the (2*S*)- and the (2*R*)-isomer, it was necessary to deplete the (2*R*)-isomer prior to addition of MCE. This was done by a 5 min incubation at 37 °C with 2.8 μg of holo-MCM, prepared as described previously [7]. The assay mixture contained 50 mM potassium phosphate (pH 7), 25 mM NaCl, 2 mM $MgCl_2$, 75 μM methylmalonyl-CoA. After the initial 5 min incubation, purified MCE was added and incubation was continued for an additional 1–5 min. Reactions were terminated by the addition of 100 μL of 1 M acetic acid, and the disappearance of methylmalonyl-CoA was measured by HPLC. Conditions were as follows: solvent A, 100 mM Na^+ acetate (pH 4.6) in 10% methanol in water; solvent B, 100 mM Na^+ acetate (pH 4.6) in 90% methanol in water. The column used was a 3.9 × 150 mm NovaPak C18 column equipped with a C18 Sentry guard column; following incubation with buffer A, a linear gradient from 0 to 60% buffer B was run over 12 min at a flow rate of 1 $mL \cdot min^{-1}$. Quantification was by integration of peak areas using BREEZE software (Waters, Milford, MA, USA). The MCE activity was determined over a range of enzyme concentrations.

Generation and expression of *C. elegans* reporter gene constructs

In order to investigate the cell-specific, developmentally regulated transcription of *mce-1*, lines of transgenic nematodes were created. The basic strategy involved the insertion of several fragments of the 5′-region of *mce-1* into the multiple cloning site of the vector pPD95.77 provided by A. Fire (Carnegie Institute, Baltimore, MD, USA). The inserted promoter sequence then drives the expression of green fluorescent protein (GFP) reporter gene. The GFP coding region is then followed by translation termination and poly(A) addition signals. The putative promoter region of the *mce-1* was amplified using the expand high fidelity PCR system (Roche) with *C. elegans* genomic DNA as template and the gene specific oligonucleotides 8060 5′-CTAGTCTA GAATTTTCTTC TCTACCACCACTG-3′ (sense, 3326 bp upstream of the translation start site) and 8071 5′-GGCCAATCCCGGGGAAACAGCTTCATGAATATC ACGAAC-3′ (antisense, in exon III); to obtain cytosolic GFP-expression, the oligonucleotide 2201 5′-GCCATTC CCGGGGCCATTTTCAAAAGAAGAATCTAT-3′ (antisense, 5′ directly preceding the translational start site of *mce-1*) was used. For microinjection, the plasmid DNA was prepared using the Endo Free Plasmid Maxi Kit (Qiagen, Hilden, Germany).

Worms used for mitochondrial colocalization experiments were grown in the dark on NGM agar plates containing MitoTracker Red CMXRos (1 $\mu g \cdot mL^{-1}$, Molecular Probes, Karlsruhe, Germany).

Microinjection

Germline transformation was carried out using *C. elegans* *pha-1(e2123)* mutants. The *pha-1*/pBX system (a kind gift from R. Schnabel, Technical University of Braunschweig, Germany) is based on the temperature-sensitive embryonic lethal mutation *pha-1*. The fusion construct (80 $\mu g \cdot ml^{-1}$) was microinjected into the distal arm of the hermaphrodite gonad as described previously [45]. The pBX plasmid that

contained a wild-type copy of the *pha-1* gene was coinjected with the fusion construct [46]. Following microinjection, the animals were transferred to 25 °C. In transgenic animals carrying the pBX plasmid, the embryo lethality caused by the *pha-1* mutation is complemented. Thus, transgenic animals can be selected by shifting the F1 larvae of injected hermaphrodites from 15 °C to 25 °C. Only transformed progeny survive this selection and can be maintained by cultivation at 25 °C. For each construct, phenotypes of multiple animals from at least three independent lines were examined using Nomarski optics.

RNA-mediated interference (RNAi)

RNAi was performed as described in an established protocol [47]. Briefly, double-stranded RNA was produced in HT115 *E. coli* strain transformed with pPD129.36 containing a 300 bp cDNA fragment starting directly after the 5′spliced leader (SL1) sequence (Fig. 3; nucleotides 23–325). Isopropyl thio-β-D-galactoside (1 mM) was added to the media and agar plates to induce transcription of the double stranded RNA. L4-staged hermaphrodites were placed onto the plates and their progeny were evaluated.

Analyses of mce-1(ok243) mutant

The mutant strain RB512 (Caenorhabditis Genetics Center, University of Minnesota, MN, USA) was kindly provided by G. Moulder of the *C. elegans* gene knockout consortium. Worm libraries mutated with trimethylpsoralen and UV irradiation were screened for a deletion mutation. After chemical mutagenesis, PCR with nested primers was used to identify animals in the mutated population with deletions at the targeted locus. PCR on single worms was carried out according to Jansen *et al.* [48]. Homozygous animals were obtained and the exact deletion site was determined by sequencing the resulting PCR fragment.

Stress resistance assays

The survival assays were performed in M9 medium at 20 °C for the given time period using ELISA plates with 10 worms per well. The animals were incubated with the stressors *t*-butylhydrogenperoxide, glucose/glucose oxidase and propionic acid. The survival rate of the *mce-1* mutants was compared to the wild-type worm culture. The mean values were calculated from four independent experiments each with at least three survival assays using worms from different generations. To exclude the possible effect of the solvents used, controls with equal amounts of solvent were performed. Furthermore, controls using only the enzyme (glucose oxidase) or substrate (glucose) were performed (data not shown). A worm was scored as dead when it did not respond to a mechanical stimulus.

Acknowledgements

This work was supported by the Deutsche Forschungsgemeinschaft (Li 793/2–1). We thank Bärbel Bergmann for help with figures. Some strains were supplied by the *Caenorhabditis* Genetics Center, which is funded by the NIH National Center for Research Sources.

References

1 Armstrong RN (2000) Mechanistic diversity in a metalloenzyme superfamily. *Biochemistry* **39**, 13625–13632.
2 Babbitt PC & Gerlt JA (1997) Understanding enzyme superfamilies. *J Biol Chem* **272**, 30591–30594.
3 Gerlt JA & Babbitt PC (2001) Divergent Evolution of enzymatic function: Mechanistically diverse superfamilies and functionally distinct superfamilies. *Annu Rev Biochem* **70**, 209–246.
4 Fenton WA & Rosenberg LE (1995) Disorders of propionate and methylmalonate metabolism. In *The Metabolic and Molecular Bases of Inherited Disease*, Vol. 2. (Scriver CR, Beaudet AL, Sly WS & Valle D, eds), pp. 1423–1449. McGraw-Hill, New York.
5 Brusque AM, Borba RR, Schuck PF, Dalcin KB, Ribeiro CA, Silva CG, Wannmacher CM, Dutra-Filho CS, Wyse AT, Briones P & Wajner M (2002) Inhibition of the mitochondrial respiratory chain complex activities in rat cerebral cortex by methylmalonic acid. *Neurochem Int* **40**, 593–601.
6 Kolker S, Schwab M, Horster F, Sauer S, Hinz A, Wolf NI, Mayatepek E, Hoffmann GF, Smeitink JA & Okun JG (2003) Methylmalonic acid, a biochemical hallmark of methylmalonic acidurias but no inhibitor of mitochondrial respiratory chain. *J Biol Chem* **278**, 47388–47393.
7 Bobik TA & Rasche ME (2001) Identification of the human methylmalonyl-CoA racemase gene based on the analysis of prokaryotic gene arrangements: implications for decoding the human genome. *J Biol Chem* **276**, 37194–37198.
8 Dayem LC, Carney JR, Santi DV, Pfeifer BA, Khosla C & Kealey JT (2002) Metabolic engineering of a methylmalonyl-CoA mutase-epimerase pathway for complex polyketide biosynthesis in *Escherichia coli*. *Biochemistry* **41**, 5193–5201.
9 Herter S, Busch A & Fuchs G (2002) L-Malyl-coenzyme A lyase/beta-methylmalyl-coenzyme A lyase from *Chloroflexus aurantiacus*, a bifunctional enzyme involved in autotrophic CO(2) fixation. *J Bacteriol* **184**, 5999–6006.
10 Korotkova N, Chistoserdova L, Kuksa K & Lidstrom ME (2002) Glyoxylate regeneration pathway in the methylotroph M*ethylobacterium extorquens* AM1. *J Bacteriol* **184**, 1750–1758.

11 Pfeifer BA & Khosla C (2001) Biosynthesis of polyketides in heterologous hosts. *Microbiol Mol Biol Rev* **65**, 106–118.
12 Watanabe K, Rude MA, Walsh CT & Khosla C (2003) Engineered biosynthesis of an ansamycin polyketide precursor in *Escherichia coli*. *Proc Natl Acad Sci USA* **100**, 9774–9778.
13 Altschul SF, Madden TL, Schaffer AA, Zhang J, Zhang Z, Miller W & Lipman DJ (1997) Gapped BLAST and PSI-BLAST: a new generation of protein database search programs. *Nucleic Acids Res* **25**, 3389–3402.
14 Harris TW, Chen NS, Cunningham F, Tello-Ruiz M, Antoshechkin I, Bastiani C, Bieri T, Blasiar D, Bradnam K, Chan J *et al*. (2004) WormBase: a multi-species resource for nematode biology and genomics. *Nucleic Acids Res* **32**, D411–D417.
15 Harris TW, Lee R, Schwarz E, Bradnam K, Lawson D, Chen W, Blasier D, Kenny E, Cunningham F, Kishore R *et al*. (2003) WormBase: a cross-species database for comparative genomics. *Nucleic Acids Res* **31**, 133–137.
16 Stein L, Mangone M, Schwarz E, Durbin R, Thierry-Mieg J, Spieth J & Sternberg P (2001) WormBase: network access to the genome and biology of *Caenorhabditis elegans*. *Nucleic Acids Res* **29**, 82–86.
17 Claros MG & Vincens P (1996) MITOPROT: Prediction of mitochondrial targeting sequences. Institut für Humangenetik, Technische Universität, München and Institut für Humangenetik GSF, Forschungszentrum für Gesundheit und Umwelt, Neuherberg. http://ihg.gsf.de/ihg/mitoprot.html.
18 Claros MG & Vincens P (1996) Computational method to predict mitochondrially imported proteins and their targeting sequences. *Eur J Biochem* **241**, 779–786.
19 McCarthy AA, Baker HM, Shewry SC, Patchett ML & Baker EN (2001) Crystal structure of methylmalonyl-coenzyme A epimerase from *P. shermanii*: a novel enzymatic function on an ancient metal binding scaffold. *Structure* **9**, 637–646.
20 Bergdoll M, Eltis LD, Cameron AD, Dumas P & Bolin JT (1998) All in the family: structural and evolutionary relationships among three modular proteins with diverse functions and variable assembly. *Protein Sci* **7**, 1661–1670.
21 Fuller JQ & Leadlay PF (1983) Proton transfer in methylmalonyl-CoA epimerase from *Propionibacterium shermanii*. The reaction of (2R)-methylmalonyl-CoA in tritiated water. *Biochem J* **213**, 643–650.
22 Peters JP & Elliot JM (1984) Effects of cobalt or hydroxycobalamin supplementation on vitamin B-12 content and (S)-methylmalonyl-CoA mutase activity of tissue from cobalt-depleted sheep. *J Nutr* **114**, 660–670.
23 Dobson CM, Wai T, Leclerc D, Wilson A, Wu X, Dore C, Hudson T, Rosenblatt DS & Gravel RA (2002) Identification of the gene responsible for the cblA complementation group of vitamin B12-responsive methylmalonic acidemia based on analysis of prokaryotic gene arrangements. *Proc Natl Acad Sci USA* **99**, 15554–15559.
24 Korotkova N & Lidstrom ME (2004) MeaB is a component of the methylmalonyl-CoA mutase complex required for protection of the enzyme from inactivation. *J Biol Chem* **279**, 13652–13658.
25 Leal NA, Park SD, Kima PE & Bobik TA (2003) Identification of the human and bovine ATP: Cob (I) alamin adenosyltransferase cDNAs based on complementation of a bacterial mutant. *J Biol Chem* **278**, 9227–9234.
26 Dobson CM, Wai T, Leclerc D, Kadir H, Narang M, Lerner-Ellis JP, Hudson TJ, Rosenblatt DS & Gravel RA (2002) Identification of the gene responsible for the cblB complementation group of vitamin B12-dependent methylmalonic aciduria. *Hum Mol Genet* **11**, 3361–3369.
27 Kovachy RJ, Copley SD & Allen RH (1983) Recognition, isolation, and characterization of rat liver D-methylmalonyl coenzyme A hydrolase. *J Biol Chem* **258**, 11415–11421.
28 Reszko AE, Kasumov T, Pierce BA, David F, Hoppel CL, Stanley WC, Des Rosiers C & Brunengraber H (2003) Assessing the reversibility of the anaplerotic reactions of the propionyl-CoA pathway in heart and liver. *J Biol Chem* **278**, 34959–34965.
29 Montgomery JA, Mamer OA & Scriver CR (1983) Metabolism of methylmalonic acid in rats. Is methylmalonyl-coenzyme a racemase deficiency symptomatic in man? *J Clin Invest* **72**, 1937–1947.
30 Mazumder R, Sasakawa T, Kaziro Y & Ochoa S (1962) Metabolism of propionic acid in animal tissues. IX. Methylmalonyl coenzyme A racemase. *J Biol Chem* **237**, 3065–3068.
31 Wajner M, Latini A, Wyse AT & Dutra-Filho CS (2004) The role of oxidative damage in the neuropathology of organic acidurias: insights from animal studies. *J Inherit Metab Dis* **27**, 427–434.
32 Fontella FU, Pulrolnik V, Gassen E, Wannmacher CM, Klein AB, Wajner M & Dutra-Filho CS (2000) Propionic and 1-methylmalonic acids induce oxidative stress in brain of young rats. *Neuroreport* **11**, 541–544.
33 Lee SS, Lee RY, Fraser AG, Kamath RS, Ahringer J & Ruvkun G (2003) A systematic RNAi screen identifies a critical role for mitochondria in *C. elegans* longevity. *Nat Genet* **33**, 40–48.
34 Pettersen EF, Goddard TD, Huang CC, Couch GS, Greenblatt DM, Meng EC & Ferrin TE (2004) UCSF Chimera – a visualization system for exploratory research and analysis. *J Comput Chem* **25**, 1605–1612.
35 Berezin C, Glaser F, Rosenberg J, Paz I, Pupko T, Fariselli P, Casadio R & Ben-Tal N (2004) ConSeq: The Identification of functionally and structurally important residues in protein sequences. *Bioinformatics* **20**, 1322–1324.

36 Edgar RC (2004) MUSCLE: multiple sequence alignment with high accuracy and high throughput. *Nucleic Acids Res* **32**, 1792–1797.
37 Higgins DG, Thompson JD & Gibson TJ (1996) Using CLUSTAL for multiple sequence alignments. *Methods Enzymol* **266**, 383–402.
38 Gouy M (2004) Unrooted. http://pbil.University-lyon1.fr/software/unrooted.html
39 Torda AE, Procter JB & Huber T (2004) Wurst: a protein threading server with a structural scoring function, sequence profiles and optimized substitution matrices. *Nucleic Acids Res* **32**, W532–W535.
40 Fiser A & Sali A (2003) Modeller: generation and refinement of homology-based protein structure models. *Methods Enzymol* **374**, 461–491.
41 Vriend G (1990) WHAT IF: a molecular modeling and drug design program. *J Mol Graph* **8**, 52–56.
42 Hooft RWW, Vriend G, Sander C & Abola EE (1996) Errors in protein structures. *Nature* **381**, 272–272.
43 Luthy R, Bowie JU & Eisenberg D (1992) Assessment of protein models with three-dimensional profiles. *Nature* **356**, 83–85.
44 Clos J & Brandau S (1994) pJC20 and pJC40 – two high-copy-number vectors for T7 RNA polymerase-dependent expression of recombinant genes in *Escherichia coli*. *Protein Expr Purif* **5**, 133–137.
45 Mello C & Fire A (1995) DNA transformation. *Methods Cell Biol* **48**, 451–482.
46 Granato M, Schnabel H & Schnabel R (1994) *Pha-1*, a selectable marker for gene transfer in *C. elegans*. *Nucleic Acids Res* **22**, 1762–1763.
47 Timmons L & Fire A (2001) Ingestion of bacterially expressed dsRNAs can produce specific and potent genetic interference in *Caenorhabditis elegans*. *Gene* **263**, 103–112.
48 Jansen G, Hazendonk E, Thijssen KL & Plasterk RH (1997) Reverse genetics by chemical mutagenesis in *Caenorhabditis elegans*. *Nat Genet* **17**, 119–121.